Proteasome Inhibition Potentiates Antitumor Effects of Photodynamic Therapy in Mice through Induction of Endoplasmic Reticulum Stress and Unfolded Protein Response

Angelika Szokalska,[1] Marcin Makowski,[1] Dominika Nowis,[1] Grzegorz M. Wilczyński,[2,3] Marek Kujawa,[2] Cezary Wójcik,[4] Izabela Młynarczuk-Biały,[2] Pawel Salwa,[1] Jacek Bil,[1] Sylwia Janowska,[1] Patrizia Agostinis,[5] Tom Verfaillie,[5] Marek Bugajski,[1] Jan Gietka,[1] Tadeusz Issat,[1] Eliza Głodkowska,[1] Piotr Mrówka,[1] Tomasz Stoklosa,[1] Michael R. Hamblin,[6] Paweł Mróz,[6] Marek Jakóbisiak,[1] and Jakub Golab[1]

Departments of [1]Immunology and [2]Histology and Embryology, Center of Biostructure Research, Medical University of Warsaw; [3]Laboratory of Molecular and Systemic Neuromorphology, M. Nencki Institute of Experimental Biology, Warsaw, Poland; [4]Department of Anatomy and Cell Biology, Indiana University School of Medicine-Evansville, Evansville, Indiana; [5]Department of Molecular and Cell Biology, Catholic University of Leuven, Campus Gasthuisberg, Leuven, Belgium; and [6]Department of Dermatology, Harvard Medical School and Wellman Center for Photomedicine, Massachusetts General Hospital, Boston, Massachusetts

Abstract

Photodynamic therapy (PDT) is an approved therapeutic procedure that exerts cytotoxic activity toward tumor cells by inducing production of reactive oxygen species such as singlet oxygen. PDT leads to oxidative damage of cellular macromolecules, including proteins that undergo multiple modifications such as fragmentation, cross-linking, and carbonylation that result in protein unfolding and aggregation. Because the major mechanism for elimination of carbonylated proteins is their degradation by proteasomes, we hypothesized that a combination of PDT with proteasome inhibitors might lead to accumulation of carbonylated proteins in endoplasmic reticulum (ER), aggravated ER stress, and potentiated cytotoxicity toward tumor cells. We observed that Photofrin-mediated PDT leads to robust carbonylation of cellular proteins and induction of unfolded protein response. Pretreatment of tumor cells with three different proteasome inhibitors, including bortezomib, MG132, and PSI, gave increased accumulation of carbonylated and ubiquitinated proteins in PDT-treated cells. Proteasome inhibitors effectively sensitized tumor cells of murine (EMT6 and C-26) as well as human (HeLa) origin to PDT-mediated cytotoxicity. Significant retardation of tumor growth with 60% to 100% complete responses was observed *in vivo* in two different murine tumor models (EMT6 and C-26) when PDT was combined with either bortezomib or PSI. Altogether, these observations indicate that combination of PDT with proteasome inhibitors leads to potentiated antitumor effects. The results of these studies are of immediate clinical application because bortezomib is a clinically approved drug that undergoes extensive clinical evaluations for the treatment of solid tumors. [Cancer Res 2009;69(10):4235–43]

Introduction

Reactive oxygen species (ROS) and, in particular, singlet oxygen ($^1O_2$) are responsible for the cytotoxic effects induced by photodynamic therapy (PDT; refs. 1, 2). $^1O_2$ reacts with proteins, lipids, and DNA (3–7). Radical-induced protein modifications include fragmentation, multimerization, misfolding, and/or structural alterations, resulting in functional inactivation, changes in mechanical properties, aggregation, formation of further reactive species, or accelerated degradation (8).

Multiple mechanisms have evolved to interact with oxidants to form less reactive products. These include enzymes that directly react with ROS such as superoxide dismutases, catalase, glutathione peroxidase, and a number of secondary scavengers participating in the reduction of oxidized biomolecules. However, during robust oxidative stress conditions, such as those occurring during PDT, these cytoprotective mechanisms are insufficient and a significant damage to cellular constituents may ensue. Therefore, other mechanisms have developed to enable restoration of normal protein function within cells. Oxidized proteins, which lose their physiologic function due to conformational changes, can be refolded by molecular chaperones such as heat shock proteins (HSP). Notably, PDT was found to induce expression of a variety of HSPs including HS1, HSP27, HSP60, HSP70, HSP90, GRP78, and GRP94, and for some of these proteins a protective role in PDT-treated cells has been shown (9–13). Inefficient restoration of protein structure that leads to accumulation of misfolded proteins within endoplasmic reticulum (ER) is called ER stress (14).

ER stress triggers several independent adaptive responses collectively referred to as unfolded protein response (UPR). Its function is to reestablish protein homeostasis and normal ER function. UPR triggers at least three signaling pathways: activation of protein kinase RNA–like ER kinase, activating transcription factor 6, and inositol-requiring enzyme 1 (15). Activation of inositol-requiring enzyme 1 leads to unusual cytosolic splicing of mRNA for X-box binding protein 1 (XBP-1), which on translation produces sXBP-1, an active transcription factor. UPR-induced genes encode chaperones (including numerous HSPs), enzymes that participate in red-ox reactions and management of oxidative stress, and genes for ER-associated degradation (ERAD). ERAD involves the retrograde translocation of unfolded proteins from the lumen of the ER to the cytosol, where they undergo degradation

Note: Supplementary data for this article are available at Cancer Research Online (http://cancerres.aacrjournals.org/).

A. Szokalska, M. Makowski, and D. Nowis contributed equally to this work.

Requests for reprints: Jakub Golab, Department of Immunology, Center of Biostructure Research, Medical University of Warsaw, 1A Banacha Street, F Building, 02-097 Warsaw, Poland. Phone: 48-22-5992199; Fax: 48-22-5992194; E-mail: jakub.golab@wum.edu.pl.

doi:10.1158/0008-5472.CAN-08-3439

in proteasomes (16). The latter are large multisubunit protease complexes endowed with three main proteolytic activities: trypsin-like, chymotrypsin-like, and caspase-like (17, 18). Excessive ER stress or a failure of UPR to counteract it can trigger cell death.

One of the typical biomarkers for oxidative protein damage is carbonylation. Carbonylation leads to exposure of hydrophobic patches within proteins, resulting in their partial unfolding, which favors their ubiquitination followed by recognition and degradation by proteasomes (19). The ubiquitin-proteasome system (UPS) has been shown to play an important cytoprotective role through degradation of oxidatively modified proteins (19, 20). Robust carbonylation of proteins results in the formation of large protein aggregates or "aggresomes," which entrap elements of the UPS, decreasing the cellular capacity of proteasomal proteolysis (21). Treatment with proteasome inhibitors is also associated with formation of intracellular protein aggregates, increased ER stress, and UPR induction in different tumor models (22, 23).

It was previously shown that PDT with purpurin-18 induces protein carbonylation in tumor cells (24). However, the fate of carbonylated proteins in tumor cells has not been investigated. Therefore, we decided to study the proteasome-mediated degradation of PDT-induced protein carbonyls to better understand the mechanisms of PDT-mediated cytotoxicity and to find out whether inhibition of this degradation would affect the antitumor effects of PDT.

Materials and Methods

Tumor cells. Human cervical cancer (HeLa) and murine breast carcinoma (EMT6) cell lines were purchased from American Type Culture Collection. Murine colon adenocarcinoma (C-26) was obtained from Dr. Danuta Dus (Institute of Immunology and Experimental Medicine, Wroclaw, Poland). HeLa cells stably expressing HA-tagged δCD3, HA-tagged αTCR, α1-antitrypsin Hong Kong mutant (α1AT), and $Ub_{G76V}GFP$ were used. Expression plasmids encoding reporter substrates were obtained from Dr. Allan Weissman (Laboratory of Protein Dynamics and Signaling, National Cancer Institute, Frederick, MD; δCD3), Dr. Kazuhiro Nagata (Department of Molecular and Cellular Biology, Kyoto University, Kyoto, Japan; α1AT), Dr. Ron Kopito (Department of Biology, Stanford University, Stanford, CA; αTCR), and Dr. Maria Masucci (Department of Cell and Molecular Biology, Karolinska Institutet, Stockholm, Sweden; $Ub_{G76V}GFP$), and their sequences were verified before transfection. Stably transfected HeLa clones expressing reporter substrates were chosen for experiments. Cells were cultured in RPMI 1640 (C-26) or DMEM (HeLa and EMT6) supplemented with 10% fetal bovine serum (Invitrogen), antibiotic/antimycotic solution (Sigma), and 400 μg/mL geneticin (Sigma; transfected HeLa cells) to ensure stable expression of plasmid vectors.

Mice. BALB/c mice, 8 to 12 wk of age, were used in the experiments. Breeding pairs were obtained from the Animal House of the Polish Academy of Sciences, Medical Research Center (Warsaw, Poland). All *in vivo* experiments were done in accordance with the guidelines approved by the Ethical Committee of the Medical University of Warsaw.

Reagents. Photofrin (Axcan Pharma, Inc.), verteporfin (a generous gift of QLT PhotoTherapeutics, Inc.), aminolevulinic acid (Sigma), and hypericin (prepared, purified, and stored as described; ref. 25) were used as photosensitizers. MG132 and PSI were purchased from Calbiochem/EMD and were dissolved in cell culture quality DMSO (Sigma). Bortezomib (Millenium Pharmaceuticals) was dissolved in 0.9% NaCl.

Tumor treatment and monitoring. Exponentially growing EMT6 and C-26 cells were harvested, resuspended in PBS, and injected into the footpad of the right hind limb of experimental mice. Tumor cell viability, measured by trypan blue exclusion, was >98%. Tumor treatment was started when all mice developed tumors with a minimum size of 3 × 4 mm.

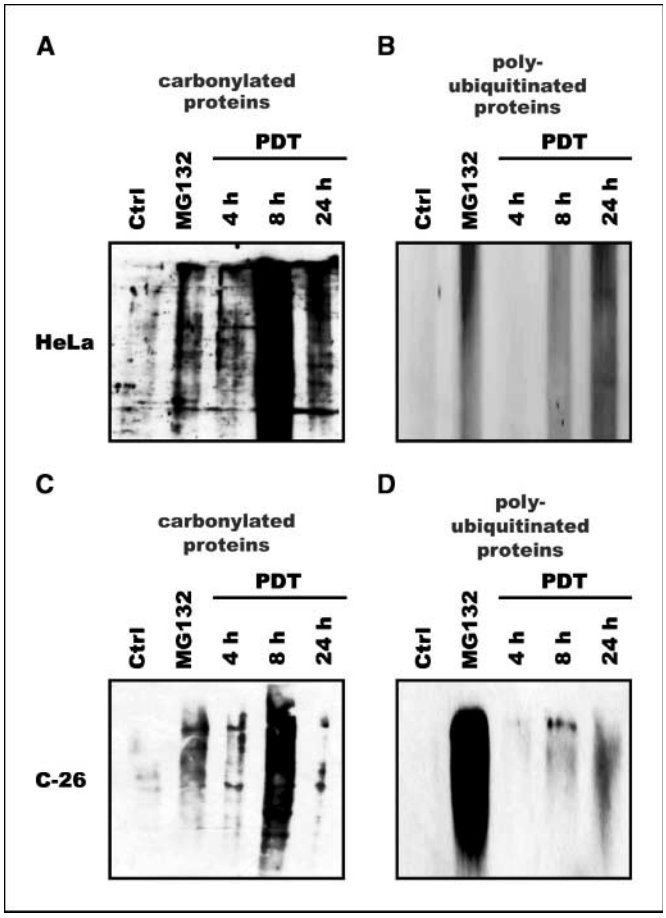

Figure 1. Influence of PDT on carbonylation and ubiquitination of cellular proteins. HeLa cells (*A*) or C-26 cells (*C*) were incubated with 10 μg/mL Photofrin for 24 h and exposed to 2.4 J/cm^2 light. At indicated time points, tumor cells were collected, and protein carbonylation was determined by the 2,4-dinitrophenylhydrazine (DNPH) method. MG132 at 250 nmol/L concentration was used as a positive control. HeLa cells (*B*) or C-26 cells (*D*) were incubated with 10 μg/mL Photofrin for 24 h and exposed to 2.4 J/cm^2 light. At indicated time points, total cell lysates were prepared from tumor cells, and Western blot analysis was done with anti-ubiquitin antibodies. MG132 at 250 nmol/L concentration was used as a positive control.

Photofrin (in 5% dextrose) was administered i.p. at a dose of 10 mg/kg 24 h before illumination with 632.8-nm light (day 6 after inoculation of tumor cells). Control mice received 5% dextrose. The light source was a He-Ne ion laser. The light at a fluence rate of 40 mW/cm^2 was delivered on day 7 of the experiments using a fiber optic light delivery system as previously described (26, 27). The total light dose delivered to the tumors was 90 J/cm^2. During illumination, mice were anesthetized with ketamine (87 mg/kg) and xylazine (13 mg/kg) and were restrained in a specially designed holder at 37°C. PSI at a dose of 20 nmol (dissolved in DMSO) was administered intratumorally (i.t.) for 7 consecutive days, with the first dose given on day 7 of the experiment. Control animals received DMSO. Bortezomib at a dose of 1 mg/kg was administered i.p. in two different schedules: on days 5 and 7 after inoculation of tumor cells (before PDT) or on days 7, 9, 11, and 13 after inoculation of tumor cells (after PDT). Control mice received 0.9% NaCl i.p. Local tumor growth was determined with calipers as previously described (28, 29) with the following formula: tumor volume (mm^3) = (longer diameter) × (shorter diameter)^2.

Statistical analyses. Data were calculated using Microsoft Excel 2007. Differences in *in vitro* cytotoxicity assays and tumor volume were analyzed for significance by Student's *t* test. Kaplan-Meier plots were generated using days of animal death (after inoculation of tumor cells) as a criterion, and survival time of animals was analyzed for significance by log-rank survival

analysis. Significance was defined as two-sided $P < 0.05$. The nature of the interaction observed between proteasome inhibitors and PDT was analyzed using the Calcusyn software (Biosoft), which uses the combination index method of Chou and Talalay (30) based on multiple drug effect equation. The advantage of this method is the automatic construction of a fraction-affected combination index table, graph, and calculation of dose reduction indices by the software. Combination indices of <1 indicate greater than additive effects (synergism; the smaller the value, the greater the degree of synergy); combination indices equal to 1 indicate additivity; and combination indices of >1 indicate antagonism.

Additional procedures are described in Supplementary Materials and Methods.

Results

PDT induces carbonylation and accumulation of ubiquitinated proteins. Time course experiments with approximately equitoxic light fluencies revealed that PDT led to a robust protein carbonylation detectable 8 hours after illumination of HeLa and C-26 cells (Fig. 1*A* and *C*). Increased protein carbonylation coincided with the accumulation of polyubiquitinated proteins at 8 hours after illumination (Fig. 1*B* and *D*). However, despite a decrease in the amount of carbonylated proteins in cellular lysates, there was a further accumulation of polyubiquitinated proteins 24 hours after illumination.

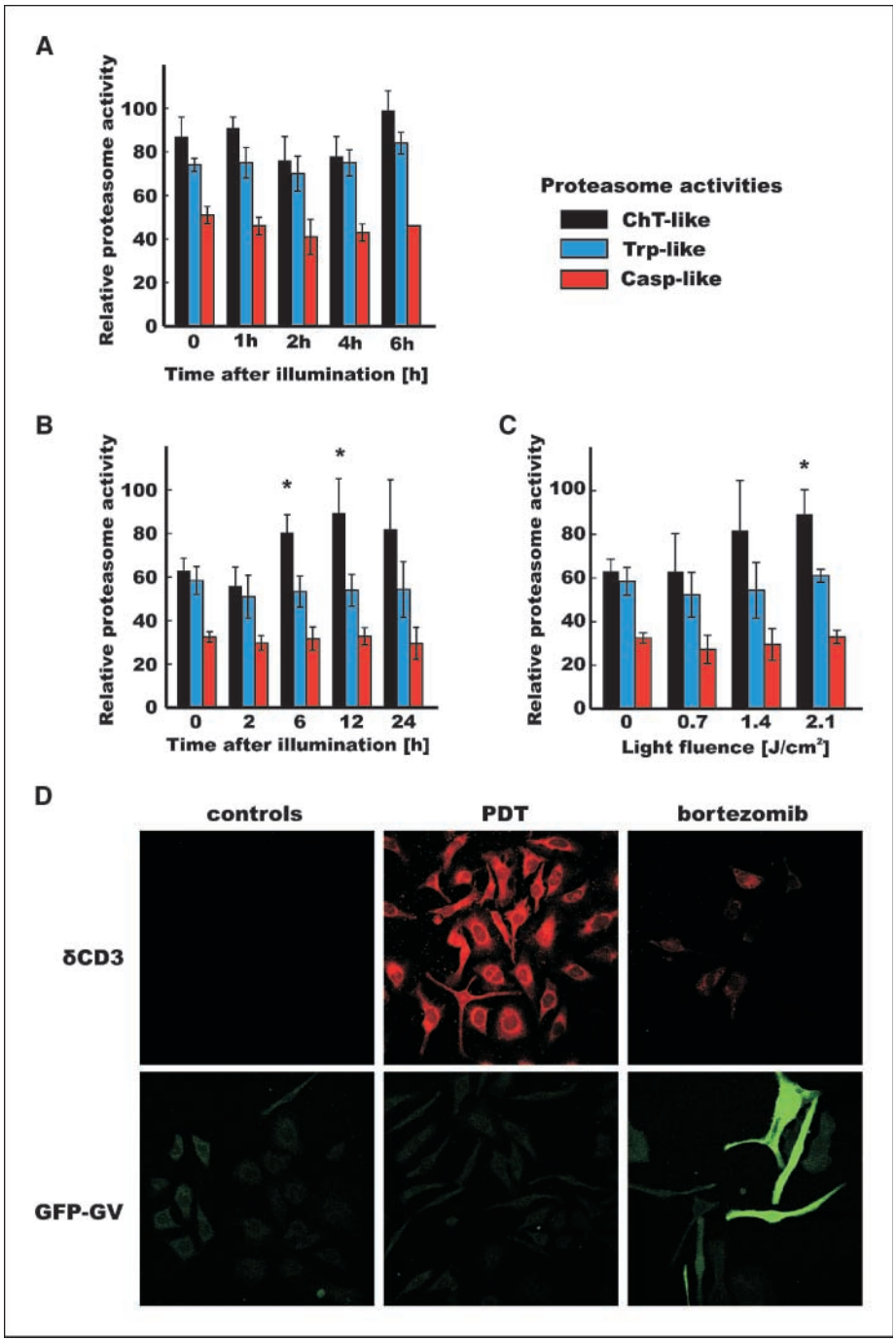

Figure 2. Influence of PDT on proteasome activity and degradation of ER-associated proteins. *A,* purified proteasome subunits were incubated for 30 min with 10 μg/mL Photofrin and illuminated with laser light at a fluence of 2.4 J/cm^2. Chymotrypsin-like (*ChT-like*), trypsin-like (*Trp-like*), and caspase-like (*Casp-like*) activities were measured with fluorogenic substrates. Relative proteasome activity represents the fluorescence intensity per microgram of protein. *B,* C-26 cells were incubated with 10 μg/mL Photofrin for 24 h and exposed to 1.4 J/cm^2 light. At indicated time points, tumor cells were collected, and proteasome activities measured in whole tumor cell lysates using fluorogenic substrates. *C,* C-26 cells were incubated with 10 μg/mL Photofrin for 24 h and exposed to indicated light fluencies. Proteasome activities were measured in whole tumor cell lysates collected 24 h after illumination using fluorogenic substrates. *D,* HeLa cells stably transfected with expression plasmids encoding reporter proteins (δCD3 and GFP-GV) were incubated with 4 ng/mL bortezomib or 10 μg/mL Photofrin for 24 h and exposed to 2.4 J/cm^2 light. Indirect immunofluorescence microscopy was done using a laser-scanning confocal microscope 24 h after illumination with anti–HA-tag (to detect δCD3) and anti-GFP primary antibodies.

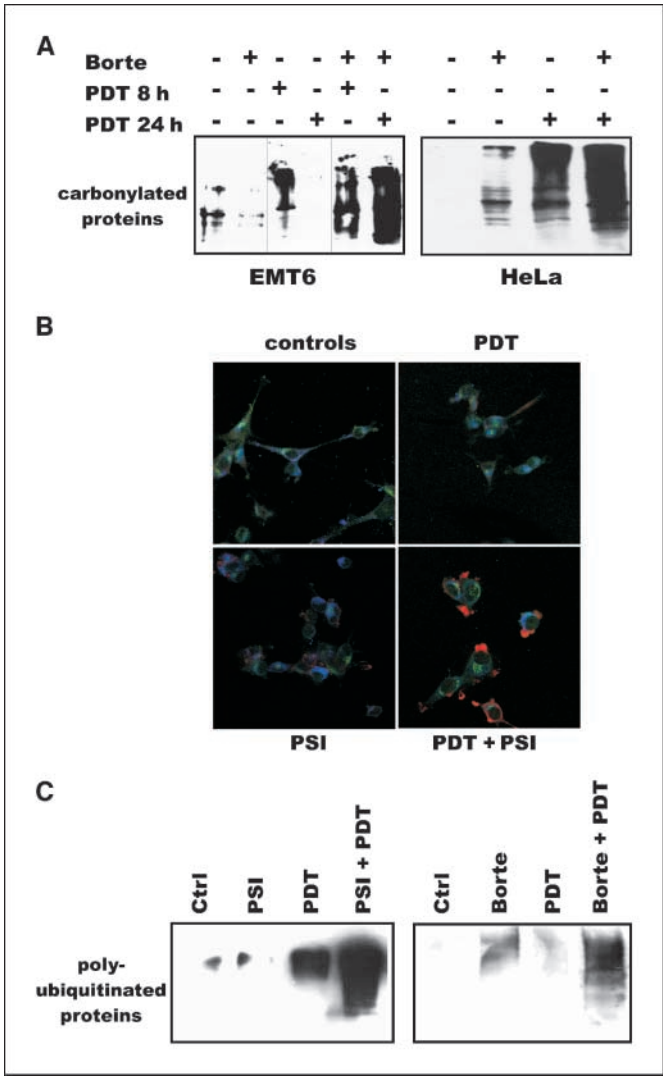

Figure 3. Proteasome inhibitors increase the accumulation of carbonylated and polyubiquitinated proteins in PDT-treated cells. *A,* EMT6 and HeLa cells were incubated with 10 μg/mL Photofrin and/or 4 ng/mL bortezomib (*Borte*) for 24 h and exposed to 1.2 J/cm^2 light. At indicated time points, tumor cells were collected and protein carbonylation was determined with DNPH. *B,* EMT6 cells were incubated with 10 μg/mL Photofrin and/or 20 nmol/L PSI for 24 h and exposed to 1.2 J/cm^2 light. Indirect immunofluorescence microscopy was done using a fluorescence microscope 24 h after illumination with anti-ubiquitin (*red*) and anti-Sec61α (*green*) primary antibodies and 4′,6-diamidino-2-phenylindole staining (*blue*). *C,* EMT6 cells were incubated with 10 μg/mL Photofrin, 20 nmol/L PSI, and/or 4 ng/mL bortezomib for 24 h and exposed to 1.2 J/cm^2 light. Total cell lysates were prepared from tumor cells 24 h after illumination, and Western blot analysis was done with anti-ubiquitin antibodies.

To study the influence of photosensitization on proteasome activity, purified 20S proteasome complexes were incubated with Photofrin and illuminated with laser light. PDT did not affect the trypsin-, chymotrypsin-, or caspase-like activities of purified proteasomes (Fig. 2*A*). However, despite the lack of direct effect of photosensitization on proteasome activity, there was a time-dependent (Fig. 2*B*) and dose-dependent (Fig. 2*C*) induction of chymotrypsin-like activity of proteasomes in whole-cell lysates of PDT-treated C-26 cells. These observations indicate that PDT does not inhibit the activity of proteasomes (found in extramembranous compartments of cells). The increased activity of proteasomes in PDT-treated cells might be an adaptive mechanism to remove oxidatively damaged proteins.

To investigate subcellular localization of photodamaged and polyubiquitinated proteins, we used two HeLa cells stably transfected with reporter constructs: an ER membrane–associated model protein (HA-tagged δCD3 chain) and a cytosolic Ub_{G76V}GFP protein (GFP-GV). Most δCD3 resides on the cytosolic side of the ER membrane and is a substrate for the ERAD pathway. GFP-GV is a cytosolic protein that has a noncleavable ubiquitin fused in frame with green fluorescent protein (GFP) that targets the protein for degradation through the ubiquitin-fusion degradation pathway. Photofrin-mediated PDT induced accumulation of ER-associated δCD3, but not cytosolic GFP-GV proteins (Fig. 2*D*). Because Photofrin is a hydrophobic photosensitizer that accumulates in membrane compartments (31), it is likely that PDT is inducing a selective damage to membrane-associated proteins that leads to ER overloading and thereby impairment of ERAD.

Oxidative damage and impaired degradation of ER-associated proteins might lead to ER stress. Indeed, PDT increased the expression of BiP and calnexin in HeLa cells (Supplementary Fig. S1*A* and *B*); reverse transcription-PCR revealed that PDT induced a time-dependent unconventional cytosolic splicing of XBP-1 (Supplementary Fig. S1*C*); and electron microscopy studies revealed that PDT led to widening of the ER lumen and to occasional vacuolization of the cytoplasm of EMT6 cells. These changes were accompanied by mitochondrial swelling and formation of infrequent lysosomal vacuoles that could represent autophagosomal vesicles (Supplementary Fig. S2). Similar changes were noticed in PDT-treated HeLa cells (see below).

Preincubation of tumor cells with proteasome inhibitors augments accumulation of carbonylated and polyubiquitinated proteins. Cells remove carbonylated proteins to avoid the toxic effects of protein aggregation by directing them for proteasome-mediated degradation (32, 33). Therefore, we examined whether inhibition of proteasomal protein degradation would affect the amount of carbonylated proteins in PDT-treated tumor cells. EMT6 cells were preincubated with bortezomib and Photofrin for 24 hours and illuminated at a fluence of 2.4 J/cm^2. A marked accumulation of carbonylated proteins was observed within 8 hours after PDT, which significantly decreased during the next 16 hours (Fig. 3*A*). In the presence of bortezomib, the amount of carbonylated proteins was higher at 8 hours after illumination, and their amount further increased during the next 16 hours. Similar effects were detected in HeLa cells (Fig. 3*A*). Immunofluorescence studies also revealed increased accumulation of polyubiquitinated proteins in cells treated with PDT + proteasome inhibitors (Fig. 3*B*). Similarly, with Western blotting we observed that proteasome inhibitors increased the amount of polyubiquitinated proteins that accumulate in PDT-treated tumor cells (Fig. 3*C*).

Next, we performed immunofluorescence studies with HeLa cells stably transfected with ER-localized model proteins: δCD3, α1AT, and αTCR. All these proteins are ERAD substrates. In normal conditions, they undergo proteasomal degradation and are undetectable by immunofluorescence. Impairment of ERAD leads to accumulation of these proteins. α1AT is an entirely lumenal ERAD substrate (with no association to the ER membrane), whereas αTCR and δCD3 are single-span transmembrane proteins. Both bortezomib and PDT, when used alone, induced slight accumulation of reporter proteins in tumor cells, but only ER membrane–associated proteins (δCD3 and αTCR) accumulated to a significantly higher extent in HeLa cells preincubated with proteasome inhibitor and treated with PDT

(Supplementary Fig. S3*A*). Immunoprecipitation of polyubiquitinated proteins followed by immunochemical detection of carbonyl groups revealed that proteins that accumulate in the treated cells were also carbonylated (Supplementary Fig. S3*B*). Similarly, immunoprecipitated δCD3 was heavily carbonylated (Supplementary Fig. S3*C*).

Preincubation of tumor cells with proteasome inhibitors potentiates the cytotoxic effects of PDT *in vitro*. Considering that PDT induces robust oxidative protein damage followed by carbonylation, and that proteasomes participate in the degradation of carbonylated proteins, we decided to investigate the outcome of the combination treatment including PDT and proteasome inhibitors. To this end, tumor cells (EMT6, C-26, and HeLa) were preincubated with Photofrin and/or three different proteasome inhibitors (bortezomib, MG132, and PSI) for 24 hours and illuminated at fluencies that produced suboptimal rates of tumor cell death. Potentiated cytotoxic effects of the combination of PDT + proteasome inhibitors in all studied cell lines were observed (Fig. 4). The proteasome inhibitor concentrations shown are the lowest that produced potentiated cytotoxicity. At higher concentrations of bortezomib, potentiated cytotoxicity was not better than that at low doses (data not shown), indicating that it might not be necessary to use high-dose treatment to elicit maximal cytotoxic response. Chow and Talalay calculations revealed that proteasome inhibitors and PDT exert synergistic and strongly synergistic cytotoxic effects against tumor cells. Incubation of tumor cells with proteasome inhibitors did not increase Photofrin uptake (Supplementary Table S1), indicating that it is an unlikely mechanism of potentiated photosensitization.

To further study the mechanism of potentiated cytotoxicity, we incubated HeLa cells with 250 nmol/L MG132 for either 24 hours or 1 hour before illumination. A 24-hour exposure to MG132 potentiated the cytotoxic effects of PDT to a higher degree than did incubation of tumor cells for 1 hour before illumination (Supplementary Fig. S4). A significant cytotoxicity was observed already at 4 hours after illumination with 2.4 J/cm^2 in HeLa cells preincubated with MG132, whereas the cytotoxic effects of PDT alone and PDT combined with a 1-hour preincubation with MG132 were recorded 24 hours after illumination (Supplementary Fig. S5*A*). Potentiated cytotoxicity was associated with accumulation of higher amounts of carbonylated proteins in cells preincubated with 250 nmol/L MG132 for 24 hours and treated with PDT (Supplementary Fig. S5*B*). Because proteasome inhibitors induce accumulation of proteins that, under normal conditions, should be degraded (34), including misfolded proteins in the ER, it can be hypothesized that the potentiated cytotoxicity results from the accrual of misfolded and/or oxidatively damaged proteins beyond the proteasomal degradative capacity. Furthermore, the influence of proteasome inhibitors on the cytotoxic effects of PDT with different photosensitizers was evaluated. For these studies, we used photosensitizers that localize predominantly either in mitochondria (verteporfin and aminolevulinic acid) or in ER (hypericin). The ER-localizing photosensitizer hypericin was found most effective in eliciting potentiated cytotoxic effects in the combined regimen (Supplementary Fig. S6).

To gain further insight into the mechanisms of potentiated cytotoxicity of the combination treatment, electron microscopy studies were done. The most remarkable lesions observed within 8 hours of illumination in cells treated with the combination of bortezomib and PDT included robust vacuolization of the cytoplasm, with frequent lysosomal/autophagosomal vesicles and extended ER (Fig. 5).

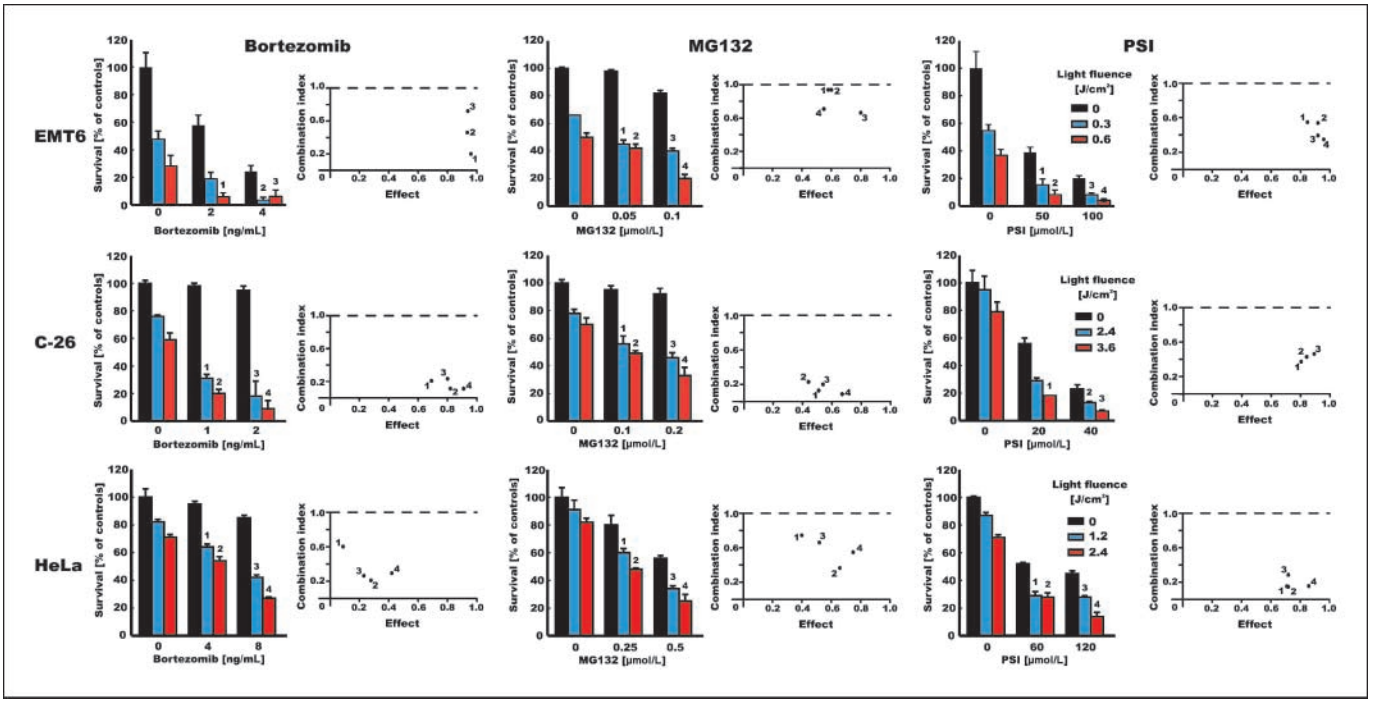

Figure 4. Proteasome inhibitors potentiate the cytotoxic effects of PDT. EMT6, C-26, and HeLa cells were incubated for 24 h with 10 μg/mL Photofrin and/or proteasome inhibitors (bortezomib, MG132, or PSI) at indicated concentrations. After 24 h of incubation, the cells were exposed to different doses of light (as indicated on the right). Following 24 h of incubation, the cytotoxic effects were measured with crystal violet staining. *Columns,* mean percent survival versus untreated controls; *bars,* SD. Next to each graph showing survival of tumor cells are the results of Chow-Talalay analyses of the combination indices, presented here as a function of inhibition of cell survival in cells treated with proteasome inhibitors and PDT (*solid circles*). Each numbered circle represents a combination on the survival graph. The straight line at combination index = 1 represents the additive effects of the two drugs.

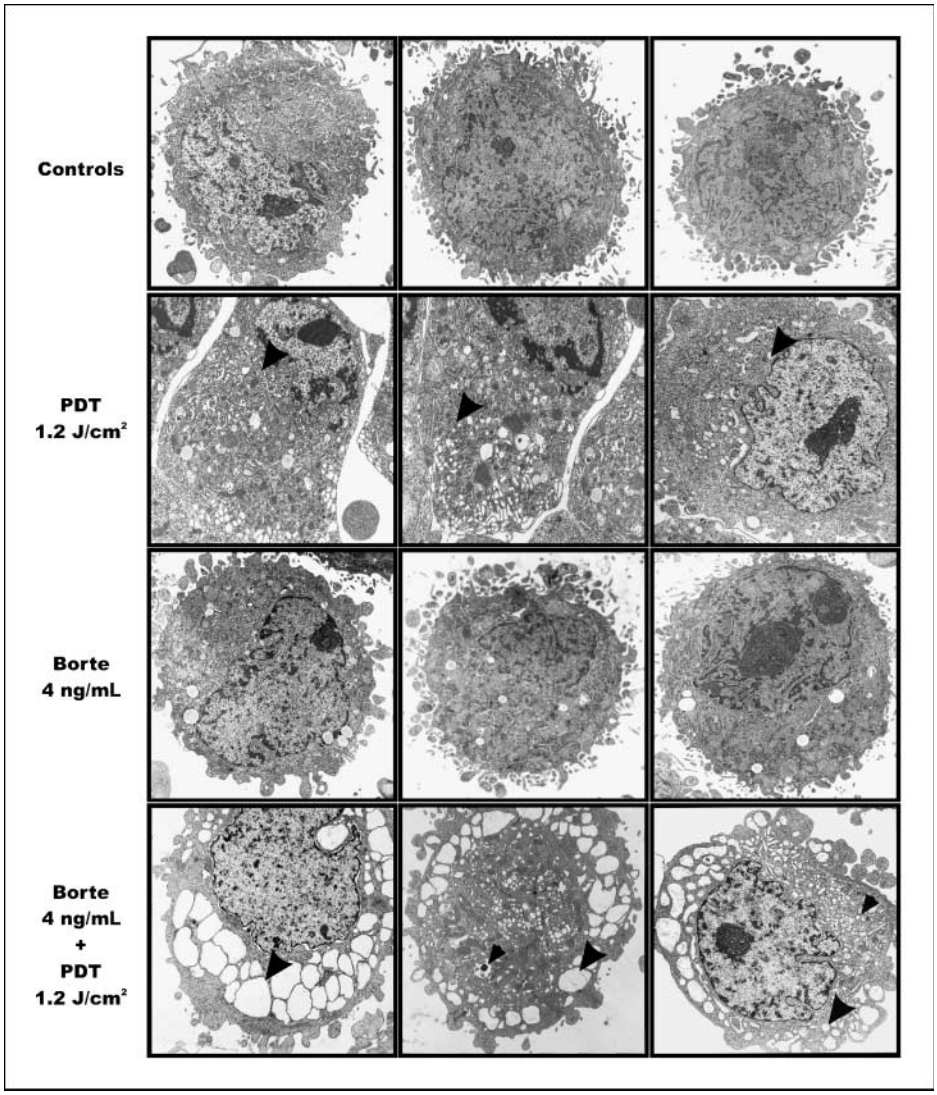

Figure 5. Electron microscopy of cells treated with PDT and/or bortezomib. HeLa cells were incubated with 10 μg/mL Photofrin and/or 4 ng/mL bortezomib for 24 h and exposed to 1.2 J/cm^2 of light. For electron microscopy, cells were collected and fixed 8 h after PDT. *Black arrowheads,* distended ER; *black arrows,* autophagosomal/lysosomal structures.

Preincubation of tumor cells with proteasome inhibitors potentiates the antitumor effects of PDT *in vivo*. In the initial *in vivo* experiment, we compared the antitumor effects of the combination treatment with bortezomib administered either before or after suboptimal PDT in an immunogenic murine breast carcinoma (EMT6) model (Fig. 6*A* and *B*). Interestingly, proteasome inhibition significantly potentiated the antitumor effects of PDT in both experimental paradigms, with complete responses observed when bortezomib was administered before or after PDT. Furthermore, PSI, another proteasome inhibitor, significantly potentiated the antitumor effects of PDT in murine colon (C-26) and breast (EMT6) adenocarcinoma models (Fig. 6*C* and *D*). Altogether, in all experiments, a marked potentiation of the antitumor effects of PDT *in vivo* was observed, resulting in retardation of tumor growth, prolongation of the survival time, and complete disappearance of tumors in at least 60% of animals (no tumor regrowth for 120 days of observation).

Discussion

It was previously shown that PDT with ER- and mitochondria-localizing purpurin-18 induces protein carbonylation, which is a typical oxidative protein modification (24). Interestingly, many of the carbonylated proteins identified in this report are normally functioning within ER and include BiP, calreticulin, phosphate disulfide isomerase, and HSP cognate 71. The major mechanism for the elimination of carbonylated proteins is their degradation by the UPS (32, 33). Therefore, we studied the influence of Photofrin-mediated PDT on carbonylation and ubiquitination of proteins. Interestingly, although the level of protein carbonylation was maximal at 8 hours after PDT and then decreased (Fig. 1*A* and *C*), the amount of polyubiquitinated proteins was still increasing until 24 hours after light exposure (Fig. 1*B* and *D*). There are several potential mechanisms for this discrepancy. It is possible that carbonylated proteins are not only ubiquitinated but are also continuously accumulating in PDT-treated cells. It is also possible that heavily carbonylated proteins are preferential substrates for proteasomes, thereby resulting in accumulation of other proteins destined for degradation. Accumulation of polyubiquitinated proteins might also be caused by impaired proteasomal degradation, as has been observed with radiotherapy (35). However, the fact that neither the function of purified 20S proteasomes after direct photosensitization nor the

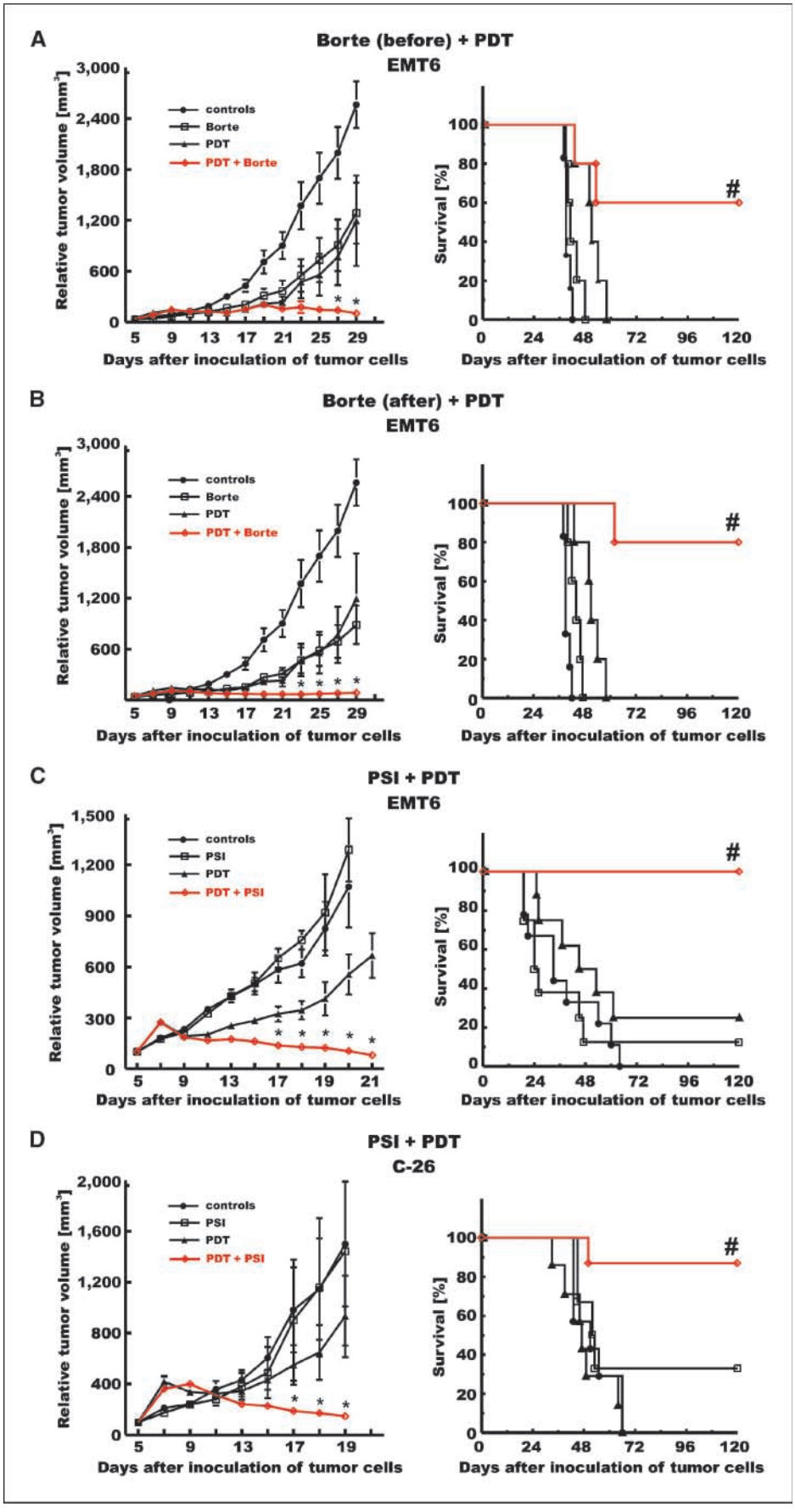

Figure 6. Antitumor effects of the combination treatment with PDT and/or proteasome inhibitors. BALB/c mice were inoculated with 1×10^5 EMT6 cells (*A*–*C*) or with 2×10^5 C-26 cells (*D*). Photofrin was administered i.p. at a dose of 10 mg/kg on day 6 (*A* and *B*) or day 5 (*C* and *D*) after inoculation of tumor cells, and 24 h later, the tumor site was illuminated with laser light at a dose of 90 J/m^2. Bortezomib was administered i.p. on days 5 and 7 (*A*) or on days 7, 9, 11, and 13 (*B*) after inoculation of tumor cells at a dose of 1 mg/kg. PSI was administered i.t. on days 6 to 12 after inoculation of tumor cells at a dose of 20 nmol/mouse (*C* and *D*). Measurements of tumor diameter were started on day 5 of the experiment and were done every 2 d. Each group consisted of five to nine animals. *, $P < 0.05$, compared with all other groups (Student's *t* test). #, $P < 0.05$, compared with all other groups (log-rank test).

proteasome activity in PDT-treated cells was impaired indicates that PDT does not damage the UPS (Fig. 2*A*–*C*). Immunofluorescence studies of HeLa cells expressing model substrates of the UPS indicated that PDT leads to selective accumulation of ER-associated reporter protein (δCD3), but not a cytosolic one (GFP-GV), although both undergo carbonylation after PDT. This observation indicates that PDT might lead to a selective impairment of the ERAD pathway, which is responsible for the retrotranslocation of damaged or misfolded proteins from the ER for their cytoplasmic degradation within proteasomes (36). Similar changes might also occur in other cellular membranes, including mitochondrial or plasma membrane, but were not further studied here.

We and others have shown that PDT leads to a rapid ROS-mediated loss of function of proteins, enzymes, and transporters colocalized in various cellular compartments with photosensitizers (37–41). For example, the ER-localizing hypericin leads to a rapid disappearance of SERCA2 Ca^{2+} transporters, which is associated with increased cytoplasmic Ca^{2+} levels (37). Rapid disappearance of SERCA2 might be caused by a number of mechanisms such as fragmentation or cross-linking, but it might also be caused by its carbonylation resulting in change of the antibody binding sites (epitopes). The possibility that PDT leads to ROS-mediated damage to the components of ERAD machinery will require further studies. It is also possible that elimination of carbonylated proteins observable within 24 hours results from engagement of other mechanisms such as autophagy. Indeed, PDT was shown to induce autophagy in tumor cells (42). Electron microscopy studies revealed that there are lysosomal/autophagosomal vesicles forming in PDT-treated cells. The potential role of autophagy in the elimination of carbonylated proteins remains to be elucidated.

Accumulation of carbonylated proteins within ER is accompanied by induction of ER stress and UPR after PDT (Supplementary Fig. S1). Although it was previously shown that PDT induces damage to ER (42–44) and increases the expression of ER chaperones (45–47), the signaling pathways associated with UPR have not been studied. We observed that PDT leads to cytoplasmic splicing of XBP-1 mRNA (Supplementary Fig. S1*C*), a transcription factor associated with UPR. Together, these observations indicate that PDT-induced damage leads to aberrant protein folding within ER. The balance between the extent of ER stress and the adaptive UPR response can dictate cell fate (14). Excessive loading of ER with unfolded proteins that results in extensive ER stress can overwhelm the capacity of UPR, leading to cell death (14, 48).

Therefore, we decided to study the cytotoxicity of a combined regimen consisting of preincubation of tumor cells with proteasome inhibitors followed by PDT. In all cell lines and combinations studied, we have observed potentiated cytotoxicity as compared with either PDT alone or proteasome inhibitor alone groups (Fig. 4). It is possible that the potentiated cytotoxicity results from accumulation of proteins within the ER membrane at the time of illumination and not from any direct interaction of PDT and proteasome inhibitors because only 24 hours, and not 1 hour, of preincubation of HeLa cells with MG132 significantly sensitized HeLa cells to PDT (Supplementary Fig. S4 and S5*A*). Combined treatment led to accumulation of more carbonylated and polyubiquitinated proteins in tumor cells as compared with single modality–treated cells (Supplementary Fig. S5*B*), and the proteins that preferentially accumulate were associated with the ER membrane (δCD3 and αTCR) but not with the ER lumen (α1AT) or cytoplasm (GFP-GV; Supplementary Fig. S3*A*). These observations indicate that most severely damaged are ER membrane–associated proteins. Indeed, transmission electron microscopy studies revealed that there is a marked vacuolization of the cytoplasm in bortezomib + PDT–treated cells (Fig. 5), which might be caused by robust extension of the ER lumen. However, it cannot be excluded that large vacuoles observed in tumor cells treated with bortezomib and PDT are of autophagic origin. In PDT-treated cells, we observed numerous swollen mitochondria (which also accumulate Photofrin), but these structures were not present in tumor cells after combination treatment. It is likely, although not further addressed, that severely damaged mitochondria were removed in a process of mitophagy.

The most important observation is that proteasome inhibitors significantly potentiate the antitumor effects of Photofrin-mediated PDT *in vivo* (Fig. 6). There were complete tumor regressions in mice treated with the combined regimen, and after 120 days of observation, tumors relapsed in only up to 40% of animals. Intriguingly, potentiated antitumor effects were observed independently of the timing of proteasome inhibitor administration and occurred when bortezomib was administered either before or after PDT. Because PDT exerts potent antivascular effects, it is possible that PDT-treated tumors undergo ischemia-reperfusion episodes that lead to prolonged oxidative stress. Therefore, administration of proteasome inhibitors before or after PDT might elicit potentiated antitumor effects that would result from either sensitization to photooxidation or postillumination oxidative stress caused by ischemia-reperfusion.

In conclusion, we observed that Photofrin-mediated PDT leads to carbonylation and ubiquitination of ER membrane–associated proteins, accompanied by induction of ER stress and UPR. Compounds that induce ER stress, such as proteasome inhibitors, can effectively sensitize tumor cells to PDT-mediated cytotoxicity. These observations are of clinical significance because proteasome inhibitors are successful drugs approved for use in oncology. However, caution should be exercised in the treatment of tumors growing at certain anatomic locations (such as esophagus, bronchi, or bladder) because potential increase in the cytotoxicity to normal cells might be associated with side effects such as perforations or bleeding.

Disclosure of Potential Conflicts of Interest

No potential conflicts of interest were disclosed.

Acknowledgments

Received 9/4/08; revised 2/23/09; accepted 3/1/09.

Grant support: Ministry of Science and Higher Education-Poland grants N40112331/2736, R0504303 (J. Golab), and N401324033 (D. Nowis); Medical University of Warsaw grants 1M19/N (M. Jakóbisiak), 1M19/WB1/07 (M. Jakóbisiak), 1M19/WB2/07 (D. Nowis), and 1M19/NM2/07 (P. Salwa); K.U.Leuven grant OT/06/49 (P. Agostinis); "Fonds voor Wetenschappelijk Onderzoek" (FWO)-Vlanderen grant G.0492.05 (P. Agostinis); U.S. NIH grant R01-CA/AI838801 (M.R. Hamblin and P. Mróz); and an institutional appropriation of the American Cancer Society grant IRG-84-002-22 (C. Wójcik). T. Issat is a recipient of the START stipend from the Foundation for Polish Science.

The costs of publication of this article were defrayed in part by the payment of page charges. This article must therefore be hereby marked *advertisement* in accordance with 18 U.S.C. Section 1734 solely to indicate this fact.

References

1. Weishaupt KR, Gomer CJ, Dougherty TJ. Identification of singlet oxygen as the cytotoxic agent in photoinactivation of a murine tumor. Cancer Res 1976;36:2326–9.
2. Juzenas P, Moan J. Singlet oxygen in photosensitization. J Environ Pathol Toxicol Oncol 2006;25:29–50.
3. Bachowski GJ, Pintar TJ, Girotti AW. Photosensitized lipid peroxidation and enzyme inactivation by membrane-bound merocyanine 540: reaction mechanisms in the absence and presence of ascorbate. Photochem Photobiol 1991;53:481–91.
4. Girotti AW. Photosensitized oxidation of cholesterol in biological systems: reaction pathways, cytotoxic effects and defense mechanisms. J Photochem Photobiol B 1992;13:105–18.
5. Davies MJ. Singlet oxygen-mediated damage to proteins and its consequences. Biochem Biophys Res Commun 2003;305:761–70.
6. Cadet J, Ravanat JL, Martinez GR, Medeiros MH, Di Mascio P. Singlet oxygen oxidation of isolated and cellular DNA: product formation and mechanistic insights. Photochem Photobiol 2006;82:1219–25.
7. Klotz LO, Kroncke KD, Sies H. Singlet oxygen-induced signaling effects in mammalian cells. Photochem Photobiol Sci 2003;2:88–94.
8. Nowis D, Golab J. Photodynamic therapy and oxidative stress. In: Hamblin MR, Mroz P, editors. Advances in photodynamic therapy: basic, translational, and clinical. Boston (MA); London: Artech House; 2008. p. 151–78.
9. Wang HP, Hanlon JG, Rainbow AJ, Espiritu M, Singh G. Up-regulation of Hsp27 plays a role in the resistance of human colon carcinoma HT29 cells to photooxidative stress. Photochem Photobiol 2002;76:98–104.
10. Jalili A, Makowski M, Switaj T, et al. Effective photoimmunotherapy of murine colon carcinoma induced by the combination of photodynamic therapy and dendritic cells. Clin Cancer Res 2004;10:4498–508.
11. Xue LY, He J, Oleinick NL. Rapid tyrosine phosphorylation of HS1 in the response of mouse lymphoma L5178Y-R cells to photodynamic treatment sensitized by the phthalocyanine Pc 4. Photochem Photobiol 1997;66:105–13.
12. Korbelik M, Sun J, Cecic I. Photodynamic therapy-induced cell surface expression and release of heat shock proteins: relevance for tumor response. Cancer Res 2005;65:1018–26.
13. Mitra S, Goren EM, Frelinger JG, Foster TH. Activation of heat shock protein 70 promoter with meso-tetrahydroxyphenyl chlorin photodynamic therapy reported by green fluorescent protein *in vitro* and *in vivo*. Photochem Photobiol 2003;78:615–22.
14. Schroder M, Kaufman RJ. The mammalian unfolded protein response. Annu Rev Biochem 2005;74:739–89.
15. Ron D, Walter P. Signal integration in the endoplasmic reticulum unfolded protein response. Nat Rev Mol Cell Biol 2007;8:519–29.
16. Romisch K. Endoplasmic reticulum-associated degradation. Annu Rev Cell Dev Biol 2005;21:435–56.
17. Wojcik C, Di Napoli M. Ubiquitin-proteasome system and proteasome inhibition: new strategies in stroke therapy. Stroke 2004;35:1506–18.
18. Golab J, Bauer TM, Daniel V, Naujokat C. Role of the ubiquitin-proteasome pathway in the diagnosis of human diseases. Clin Chim Acta 2004;340:27–40.
19. Grune T, Merker K, Sandig G, Davies KJ. Selective degradation of oxidatively modified protein substrates by the proteasome. Biochem Biophys Res Commun 2003;305:709–18.
20. Dunlop RA, Rodgers KJ, Dean RT. Recent developments in the intracellular degradation of oxidized proteins. Free Radic Biol Med 2002;33:894–906.
21. Grune T, Jung T, Merker K, Davies KJ. Decreased proteolysis caused by protein aggregates, inclusion bodies, plaques, lipofuscin, ceroid, and "aggresomes" during oxidative stress, aging, and disease. Int J Biochem Cell Biol 2004;36:2519–30.
22. Nowis D, McConnell EJ, Dierlam L, Palamarchuk A, Lass A, Wojcik C. TNF potentiates anticancer activity of bortezomib (Velcade) through reduced expression of proteasome subunits and dysregulation of unfolded protein response. Int J Cancer 2007;121:431–41.
23. Lee AH, Iwakoshi NN, Anderson KC, Glimcher LH. Proteasome inhibitors disrupt the unfolded protein response in myeloma cells. Proc Natl Acad Sci U S A 2003;100:9946–51.
24. Magi B, Ettorre A, Liberatori S, et al. Selectivity of protein carbonylation in the apoptotic response to oxidative stress associated with photodynamic therapy: a cell biochemical and proteomic investigation. Cell Death Differ 2004;11:842–52.
25. Chen B, Roskams T, Xu Y, Agostinis P, de Witte PA. Photodynamic therapy with hypericin induces vascular damage and apoptosis in the RIF-1 mouse tumor model. Int J Cancer 2002;98:284–90.
26. Golab J, Olszewska D, Mroz P, et al. Erythropoietin restores the antitumor effectiveness of photodynamic therapy in mice with chemotherapy-induced anemia. Clin Cancer Res 2002;8:1265–70.
27. Golab J, Wilczynski G, Zagozdzon R, et al. Potentiation of the anti-tumour effects of Photofrin-based photodynamic therapy by localized treatment with G-CSF. Br J Cancer 2000;82:1485–91.
28. Golab J, Kozar K, Kaminski R, et al. Interleukin 12 and indomethacin exert a synergistic, angiogenesis-dependent antitumor activity in mice. Life Sci 2000;66:1223–30.
29. Kozar K, Kaminski R, Switaj T, et al. Interleukin 12-based immunotherapy improves the antitumor effectiveness of a low-dose 5-aza-2′-deoxycitidine treatment in L1210 leukemia and B16F10 melanoma models in mice. Clin Cancer Res 2003;9:3124–33.
30. Chou TC, Talalay P. Quantitative analysis of dose-effect relationships: the combined effects of multiple drugs or enzyme inhibitors. Adv Enzyme Regul 1984;22:27–55.
31. Castano AP, Demidova TN, Hamblin MR. Mechanisms in photodynamic therapy: part three—photosensitizer pharmacokinetics, biodistribution, tumor localization and modes of tumor destruction. Photodiagn Photodyn Ther 2005;2:91–106.
32. Dalle-Donne I, Aldini G, Carini M, Colombo R, Rossi R, Milzani A. Protein carbonylation, cellular dysfunction, and disease progression. J Cell Mol Med 2006;10:389–406.
33. Nystrom T. Role of oxidative carbonylation in protein quality control and senescence. EMBO J 2005;24:1311–7.
34. Divald A, Powell SR. Proteasome mediates removal of proteins oxidized during myocardial ischemia. Free Radic Biol Med 2006;40:156–64.
35. Pajonk F, Pajonk K, McBride WH. Apoptosis and radiosensitization of Hodgkin cells by proteasome inhibition. Int J Radiat Oncol Biol Phys 2000;47:1025–32.
36. Ahner A, Brodsky JL. Checkpoints in ER-associated degradation: excuse me, which way to the proteasome? Trends Cell Biol 2004;14:474–8.
37. Buytaert E, Callewaert G, Hendrickx N, et al. Role of endoplasmic reticulum depletion and multidomain proapoptotic BAX and BAK proteins in shaping cell death after hypericin-mediated photodynamic therapy. FASEB J 2006;20:756–8.
38. Petrat F, Pindiur S, Kirsch M, de Groot H. NAD(P)H, a primary target of $^1O_2$ in mitochondria of intact cells. J Biol Chem 2003;278:3298–307.
39. Usuda J, Chiu SM, Murphy ES, Lam M, Nieminen AL, Oleinick NL. Domain-dependent photodamage to Bcl-2. A membrane anchorage region is needed to form the target of phthalocyanine photosensitization. J Biol Chem 2003;278:2021–9.
40. Xue LY, Chiu SM, Oleinick NL. Photochemical destruction of the Bcl-2 oncoprotein during photodynamic therapy with the phthalocyanine photosensitizer Pc 4. Oncogene 2001;20:3420–7.
41. Salet C, Moreno G, Ricchelli F, Bernardi P. Singlet oxygen produced by photodynamic action causes inactivation of the mitochondrial permeability transition pore. J Biol Chem 1997;272:21938–43.
42. Buytaert E, Callewaert G, Vandenheede JR, Agostinis P. Deficiency in apoptotic effectors Bax and Bak reveals an autophagic cell death pathway initiated by photodamage to the endoplasmic reticulum. Autophagy 2006;2:238–40.
43. Grebenova D, Kuzelova K, Smetana K, et al. Mitochondrial and endoplasmic reticulum stress-induced apoptotic pathways are activated by 5-aminolevulinic acid-based photodynamic therapy in HL60 leukemia cells. J Photochem Photobiol B 2003;69:71–85.
44. Kessel D, Castelli M, Reiners JJ. Ruthenium red-mediated suppression of Bcl-2 loss and Ca^{2+} release initiated by photodamage to the endoplasmic reticulum: scavenging of reactive oxygen species. Cell Death Differ 2005;12:502–11.
45. Gomer CJ, Ferrario A, Rucker N, Wong S, Lee AS. Glucose regulated protein induction and cellular resistance to oxidative stress mediated by porphyrin photosensitization. Cancer Res 1991;51:6574–9.
46. Mak NK, Li KM, Leung WN, et al. Involvement of both endoplasmic reticulum and mitochondria in photokilling of nasopharyngeal carcinoma cells by the photosensitizer Zn-BC-AM. Biochem Pharmacol 2004;68:2387–96.
47. Buytaert E, Matroule JY, Durinck S, et al. Molecular effectors and modulators of hypericin-mediated cell death in bladder cancer cells. Oncogene 2008;27:1916–29.
48. Lin JH, Walter P, Yen TS. Endoplasmic reticulum stress in disease pathogenesis. Annu Rev Pathol 2008;3:399–425.